Learning From FM Communications: Toward Accurate, Efficient, All-Terrain Vehicle Localization

Xi Chen, Qiao Xiang, *Member, IEEE*, Linghe Kong, *Senior Member, IEEE*, Huisan Xu, and Xue Liu, *Fellow, IEEE*

***Abstract*— Vehicle localization service is a fundamental component of intelligent transportation systems. The widely used satellite navigation systems perform poorly in urban areas because the lines of sight to satellites are blocked by complex terrain characteristics, *e.g.*, buildings, elevated streets and interchanges. In this paper, we design RadioLoc, a novel system achieving accurate, efficient, all-terrain vehicle localization with two key design points. First, RadioLoc harvests the frequency modulation (FM) signal, which has higher availability than satellite signal in complex terrains, as the signal source for localization. Second, RadioLoc integrates modern machine learning techniques into the processing of FM signals to efficiently learn the accurate vehicle localization in all-terrain environments. We validate the feasibility of FM-based vehicle localization and corresponding challenges and practical issues via field tests (*e.g.*, signal distortion, signal inconsistency and limited in-vehicle radio bandwidth), and develop a series of advanced techniques in RadioLoc to address them, including adaptive batching, frequency sweeping, a novel multipath delay spread filter, a reconstructive PCA denoiser and a tailored FM feature extractor. We then develop a generic, modular localization module in RadioLoc, and design different learning-based 3D position identification algorithms for this module. We implement a prototype of RadioLoc and perform extensive field experiments to evaluate its efficiency and efficacy. Results show that (1) RadioLoc achieves a real-time localization latency of less than 100 milliseconds; (2) RadioLoc achieves a worst-case localization accuracy of 99.6% even in an underground parking lot, and (3) the horizontal error of RadioLoc is only one sixth of a dedicated GPS device even when the vehicle is moving at a high-speed (*i.e.*, 80 km/h) in a complex highway scenario.**

***Index Terms*— Localization, frequency modulation (FM) communications.**

I. Introduction

VEHICLE localization is one of the most critical services in intelligent transportation systems (ITS), and the foundation of many ITS applications, such as navigation, electronic toll collection, traffic monitoring, emergency response and autonomous driving. Global Navigation Satellite Systems (GNSS), such as the Global Positioning System (GPS) [1], are the most widely used civilian vehicle localization systems. However, even being augmented by advanced technologies, the efficacy of GNSS is still constrained by an inherent limitation: GNSS requires a clear line of sight from the vehicle to at least three satellites for accurate localization. The impact of this limitation is particularly magnified in urban environments, where the line of sight is blocked by a large number of obstacles made of concrete and steel such as stack interchanges, multi-level garages, underground parking, street canyons, elevated roads and tunnels.

To cope with this limitation and achieve all-terrain vehicle localization, academia and industry have investigated the feasibility of many alternative signal sources. For example, Assisted GPS (A-GPS) [2]–[4] utilizes the assistance of cellular networks to provide localization service to smart phones under a partially blocked sky. However, the localization errors of A-GPS are substantially larger than those of dedicated GPS devices [4]. Systems using other signal sources (*e.g.*, WiFi [5]–[8], acoustic signals [9] and visible light [10], [11]) provide a high accuracy for indoor localization. However, such signals are either less available or highly dynamic for vehicles in complex terrains.

In this paper, we design RadioLoc, a novel machine learning based system that achieves accurate, efficient, all-terrain vehicle localization with two key design points. First, RadioLoc adopts the *FM radio signal*, a wireless signal highly available in all-terrain environments, as the signal source for localization. The FM signal is more advantageous over other signals (*i.e.*, satellite, cellular, WiFi, acoustic and visible light) for all-terrain vehicle localization, because it is free, highly available in complex urban terrains (*e.g.*, underground parking garages and tunnels), and requires no additional reception hardware on vehicles. More importantly, the uniqueness of FM signal fingerprints in a given geographical area has been identified and leveraged in earlier FM-assisted localization methods [12]–[15]. Second, RadioLoc integrates modern machine learning techniques into the processing of FM signals, including adaptive sampling, profile feature extraction and location computation, to efficiently generate the accurate vehicle localization in all-terrain environments.

Even with all the advantages of FM signal, the previous studies on FM-based indoor localization [12]–[14], and the recent progress of modern machine learning theories and systems [16], [17], however, realizing accurate, efficient, all-terrain vehicle localization is still *non-trivial*. For example, in an earlier attempt to use FM signal for outdoor localization [15], the average localization error is 8 km. Through field experiments in Section II, we identify a series of unique challenges. First, the multipath richness of FM radio signal propagation generates large delay spreads, leading to significant *signal distortions* around some FM station frequencies. Second, even at the same location, the power offsets and

Manuscript received 21 October 2020; revised 20 December 2021 and 3 May 2022; accepted 5 June 2022; approved by IEEE/ACM TRANSACTIONS ON NETWORKING Editor Y. Chen. Date of publication 7 July 2022; date of current version 16 February 2023. *(Xi Chen and Qiao Xiang are co-first authors.) (Corresponding author: Linghe Kong.)*

Xi Chen and Xue Liu are with the School of Computer Science, McGill University, Montreal, QC H3A 0G4, Canada (e-mail: Xi.chen11@mcgill.ca; xueliu@cs.mcgill.ca).

Qiao Xiang and Huisan Xu are with the School of Informatics, Xiamen University, Xiamen 361005, China, and also with the Tan Kah Kee Innovation Laboratory, Xiamen, Fujian 361102, China (e-mail: xiangq27@gmail.com; 22920182204327@stu.xmu.edu.cn).

Linghe Kong is with the Department of Computer Science and Engineering, Shanghai Jiao Tong University, Shanghai 200240, China (e-mail: linghe.kong@sjtu.edu.cn).

Digital Object Identifier 10.1109/TNET.2022.3187885

interference levels of FM signals could vary significantly, due to the diversities of vehicle models, weather conditions, and the manual tuning of radio power gains by users, which leads to the *inconsistency of FM signal fingerprints*. Third, the *high mobility of vehicles*, as well as the *limited bandwidth of in-vehicle radios*, further degrades the localization accuracy. Fourth, the location of vehicles needs to be computed in real-time even when vehicles are moving at a high speed.

To address these challenges, in RadioLoc, we develop multiple advanced techniques (Section III and Section IV). In particular, RadioLoc detects and eliminates the signal distortions caused by delay spreads directly (instead of estimating the delay spreads themselves), with a Mahalanobis distance based filter. A reconstructive Principle Component Analysis (rPCA) denoising technique is then designed to further reduce the residual noises. Second, to cope with the inconsistency of FM signal fingerprints, RadioLoc extracts essential signal features that are immune to diverse vehicle models and changing weather. The variations in power offsets and interference levels are neutralized. Third, RadioLoc embraces an adaptive batching technique, which adjusts the data collection periods according to the current vehicle velocity, and utilizes a frequency sweep technique to increase the system bandwidth for low-end radios. Fourth, RadioLoc develops a modular classification component, which allows the adoption of different machine learning classification algorithms for achieving accurate all-terrain localization. As a proof of concept, this paper presents a random forest based learning algorithm that can swiftly learn the accurate location of vehicles using commodity CPUs. With this modular design, we also implement a series of other learning algorithms, *e.g.*, support vector machine (SVM) and adaptive boosting (Adaboost), in RadioLoc, and compare their performances in the field. We observe that they provide similar accurate localization results. This demonstrates the modularity of RadioLoc, and the efficacy and wide applicability of the novel FM signal processing techniques developed in RadioLoc (*e.g.*, sampling, feature extraction and batching).

We implement a prototype of RadioLoc and perform extensive field experiments to evaluate its performance (Sections VI, VII and VIII). Specifically, we conducted field experiments in three complementary scenarios with different terrains - a multi-floor parking building, a street section in an open neighborhood, and two mountain tunnels. In the first scenario, results show that RadioLoc achieves a worst-case localization accuracy of 99.6% in a total of 18 locations scattering on four different floors (including one underground floor). A high-speed (*i.e.*, 80 km/h) test in the second scenario shows that RadioLoc lowers the horizontal errors to 16.7% of those given by a dedicated GPS device. In the third scenario of mountain tunnels, results show that RadioLoc achieves an average localization error less than 0.7 meter under uncontrolled driving behaviors. In all scenarios, RadioLoc achieves a localization latency of less than 100 milliseconds.

The **main contributions** of this paper are as follows.

- We design RadoiLoc, a novel FM-based vehicle localization system, which to the best of our knowledge is the first working system that achieves efficient, accurate, all-terrain vehicle localization;
- We identify the design challenges and practical issues of FM-based all-terrain vehicle localization through field tests, and develop a series of novel techniques to systematically address these issues;

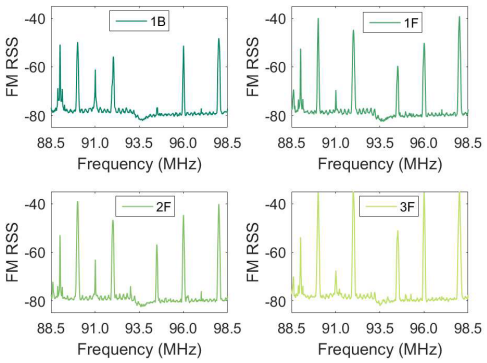

Fig. 1. FM RSS profiles of four positions.

- We fully implement RadioLoc and perform extensive field experiments, including a federated setting, to demonstrate the efficiency and efficacy of RadioLoc, in terms of localization accuracy and latency.

The remainder of the paper is organized as follows. Section II discusses the background and the design challenges of locating vehicles with FM communications. Section III gives an overview of the RadioLoc system, and Section IV presents the details of the advanced techniques we develop in RadioLoc to address the design challenges. Section V introduces the implementation details of our RadioLoc prototype. Sections VI, VII and VIII) present the results of extensive field experiments of RadioLoc. Section IX discusses the related work, and Section X concludes the paper.

II. FM-Based Vehicle Localization: Feasibility and Challenges

We identify the feasibility and corresponding challenges of FM-based all-terrain vehicle localization through field experiments in a four-floor parking building. The building has one basement $1B$ floor and three floors $1F$, $2F$ and $3F$ on the ground. We used USRP B210 boards as onboard FM radios, and left the built-in FM radios untouched to minimize the inconveniences to the volunteers.

A. Feasibility Experiments

We first parked an equipped vehicle on four different floors of the building. On each floor, this vehicle was parked at the same horizontal position. Hence, these four locations shared the same longitude and latitude, but had different altitudes. RSS profiles of FM signals were recorded at these locations. Here, an RSS profile is defined as a set of RSS values at different frequency points over a certain bandwidth. For each location, multiple samples of RSS profiles were recorded, and an average profile was calculated based on these samples.

The average RSS profiles of four different positions are illustrated in Fig. 1. In the RSS profiles, there are multiple peaks, each of which corresponds to a local radio station. It is shown that the peaks have different values and orders on different floors. These profiles are distinguishable from each other by analyzing their RSS peaks at the radio station frequencies. As such, we conclude that FM-based all-terrain vehicle localization is feasible.

B. Experimental Investigation of Challenges

Although we find that FM-based all-terrain vehicle localization is feasible, and some FM-based indoor localization

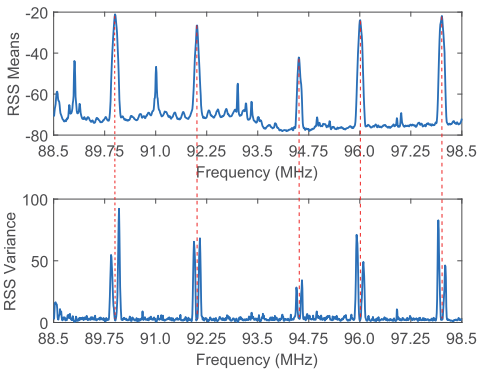

Fig. 2. Means and variances of RSS values at 1F over 200 samples.

systems are also recently developed, (*e.g.*, [12]–[14]). Many issues remain open when designing an FM-based vehicle localization system. To identify these issues, we further conduct several sets of field tests.

1) Impact of Multipath Delay Spread: The complicated urban terrain introduces a rich set of multipaths to FM radio broadcasting, leading to a large delay spread in the FM signals. This spread in the time domain introduces random and unpredictable signal dispersion in the frequency domain. To analyze the impact of the delay spread, we further study the statistical details of FM RSS profiles. Fig. 2 takes $1F$ as an example, and depicts the means and variances of RSS values over 200 samples. An interesting observation is that, while the peaks of means appear at the frequencies of radio stations (we call them station frequencies in the rest of this paper), the peaks of variances are a bit off these station frequencies. This suggests that, while the centers of FM signals are always located at station frequencies, their shapes vary dynamically. Since the vehicle was parked during the recording, these variations should be mainly introduced by the multipath reflections of FM signals. The large and time-changing delay spreads were reflected as signal distortions in the frequency domain, leading to the large variances around radio station frequencies. Therefore, we have a unique challenge summarized as follows.

Challenge 1: The multipath richness of FM signals introduces severe delay spreads, which lead to previously undiscovered noises around station frequencies.

2) Impact of Vehicle Diversity: There are numerous ground vehicle models. Each of them may have a distinct placement of radio antennas, a unique radio device, and different materials resulting in special signal propagation factors. Even vehicles from the same model may behave differently. To investigate the impact of vehicle diversity, we next employ a second vehicle from a different brand, and repeat the field tests on the same day as before. Fig. 3(b) compares the average RSS values in four different positions between two vehicles. Although both vehicles are parked at the same positions, their average RSS values are different. This suggests that the raw RSS profiles are not consistent across different vehicle setups. A closer investigation of the values reveals that there is a nearly constant power offset of $4.3dB$ between the results of the two vehicles. Therefore, we summarize the following challenge.

Challenge 2: The diversity in vehicle models may introduce variations in power-related features such as path losses and receiver-side gains. An almost constant yet unknown power offset is brought to FM signals, making their RSS profiles inconsistent.

TABLE I
RELATIVE INTERFERENCE UNDER DIFFERENT WEATHER CONDITIONS

	Sunny	Rainy	Cloudy
Interference level	-78.2	-79.8	-76.3

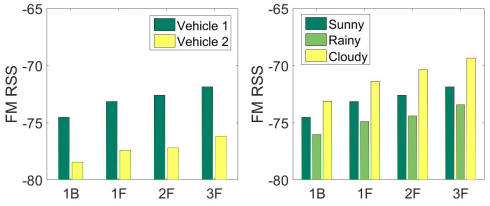

(a) With different vehicles. (b) Under different weather.

Fig. 3. FM RSS variations due to different vehicles and weather conditions.

3) Impact of Weather Conditions: Besides internal factors, the consistency of FM signals may also be affected by external factors. FM signal broadcasting could be sensitive to weather conditions. An example is the well-known rain fade phenomenon. However, we still need to understand the impact of weather conditions on FM RSS profiles and FM-assisted localization. Therefore, we repeat the tests with the first vehicle on different days under different weather conditions. Fig. 3(b) compares the average RSS values across three weather conditions. It is illustrated that the average RSS values vary with weather conditions. A further investigation reveals that the changes in interference level (Table I) contribute to these undesirable variations, leading to the following challenge.

Challenge 3: The diversity in weather conditions may introduce variations to the interference level, resulting in inconsistent FM profiles.

4) Other Practical Issues: In addition to the above challenges, there also exist other practical issues that need to be addressed.

Practical Issue 1: To cancel the white noise, it is required to collect multiple samples of RSS profiles at one location. However, when the vehicles are moving, it is impossible to gather multiple samples at exactly the same location. Instead, we may resolve to the collection of multiple samples within a small range. The size of this range may vary significantly with vehicle speed, which prevents us from obtaining consistent RSS profiles and FM fingerprints.

Practical Issue 2: The most important frequency components of RSS profiles are located at the frequencies of radio stations, which are separated by hundreds of KHz. Low-end in-vehicle radios may not have a large enough bandwidth to cover an abundant number of radio stations in RSS profiles. As a result, the resolution and accuracy of FM localization may degrade.

Practical Issue 3: Vehicle localization has strong real-time and accuracy requirements. The accurate location of vehicles needs to be computed in real-time even when vehicles are moving at a high speed.

III. RADIOLOC OVERVIEW

In this section, we give an overview of the architecture and workflow of RadioLoc, as illustrated in Fig. 4. On a high level, RadioLoc consists of three key components: *signal sampling*, *data processing*, and *location computation*.

Signal sampling. RadioLoc utilizes its radio to gather the ambient FM signals x centering at the frequency f_C. This

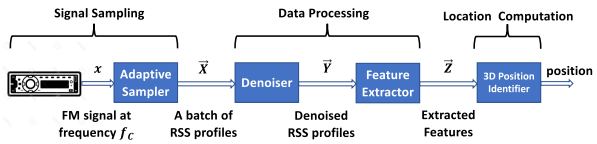

Fig. 4. Overview of RadioLoc.

center frequency is determined and adjusted by the frequency selector. Suppose the bandwidth of these frequency signals x is B. Continuous signals are converted to digital signals, and are passed to the succeeding adaptive sampler.

Upon receiving each signal sample, the adaptive sampler calculates the RSS value on each frequency point, and obtains an RSS profile $\vec{x}$ covering the bandwidth B. These profiles are output with a rate of R samples per second. This rate is the output rate of digital samples with bandwidth B, and is different from the sampling rate of FM radio. We denote each sample of RSS profiles $\vec{x}$ as

$$\vec{x} = \{x_{f_1}, \ldots, x_{f_l} \ldots, x_{f_L}\}^T, \tag{1}$$

where x_{f_l} denotes the RSS value at the lth frequency point f_l, and L is the total number of frequency points in the frequency domain. The interval between two frequency points is thus B/L Hz. Every T seconds, the sampler creates an RSS profile batch with all the RSS profiles obtained during this period. Each batch is denoted as $\vec{X} = \{\vec{x}^{(1)}, \ldots, \vec{x}^{(i)}, \ldots, \vec{x}^{(N)}\}$, where $N = RT$, and the superscript i of $\vec{x}^{(i)}$ refers to the sequential number of profiles in one batch. Each batch is then output to the succeeding block. Note that the use of this batch technique is necessary to compensate the white noise across consecutive RSS profiles. In addition to the normal batching sampling, RadioLoc also develops novel solutions, including adaptive batching and frequency sweeping, to cope with the difficulty of collecting multiple samples within a small range of location while vehicle is moving at different speeds (*i.e.*, **Practical issue 1**) and the limited bandwidth of in-vehicle radio (*i.e.*, **Practical issue 2**).

Data processing. To cope with the signal distortion caused by the multipath richness of FM signals (*i.e.*, **Challenge 1**), and the inconsistency of FM signal fingerprints caused by the vehicle and weather diversity (*i.e.*, **Challenges 2 and 3**), RadioLoc develops two novel modules to sequentially process the collected signal samples before utilizing them for localization. First, a denoiser is designed to eliminate the noises in each batch of RSS profiles $\vec{X}$, and outputs the denoised result as $\vec{Y}$. The noises to be cancelled include not only the white noise but also the signal distortions introduced by multipath delay spread. To avoid the computationally heavy estimation of delay spread, the proposed denoiser employs a Mahalanobis distance based filter to detect and remove the distorted RSS values directly. It then applies a reconstructive PCA denoising technique to further reduce the residual noises.

Second, a feature extractor is designed to eliminate the FM signal inconsistency brought by the diversities of vehicles, radios, and weather conditions. It achieves this goal by extracting FM signal features that are irrelevant to these diversities. The extractor first normalizes each denoised profile $\vec{y}^{(i)}$ in the denoised batch $\vec{Y}$, so as to compensate the unknown power offsets brought by vehicle/radio diversity. It then calculates features of each normalized RSS profile, including the heights of peaks, the order of peaks, and a binary differential sequence of the profile (to be defined in Section IV-C). These features are combined and weighted as a feature vector $\vec{z}^{(i)}$. The extractor processes all denoised profile in a batch, and outputs a batch of feature vector as $\vec{Z} = \{\vec{z}^{(1)}, \ldots, \vec{z}^{(N)}\}$.

Location computation. This component receives the extracted feature vectors $\vec{Z}$ from the feature extractor, and computes the longitude, latitude and altitude of the vehicle. In RadioLoc, we model the 3D localization of vehicle as a classification problem. The design of RadioLoc is modular so that different machine learning algorithms can be plugged in. To compute the location of vehicle in real-time (*i.e.*, **Practical issue 3**) while making the deployment of RadioLoc feasible on mainstream in-vehicle operating systems, we choose not to use learning algorithms whose performance heavily relies on specialized hardware (*e.g.*, deep learning performs much faster on GPU than on CPU). Instead, in RadioLoc, we choose to use learning algorithms whose performance are less hardware-dependent (*e.g.*, random forest, SVM and AdaBoost).

IV. RadioLoc Design Details

After an overview of the basic workflow of RadioLoc, in this section, we present the design details of RadioLoc and how the novel mechanisms address the challenges and practical issues identified in Section II.

A. Signal Sampling

As introduced in Section III, the signal sampling component in RadioLoc uses its radio to gather the ambient FM signals x centering at the frequency f_C. We denote the bandwidth of these frequency signals x as B. Continuous signals are converted to digital signals, and are passed to the succeeding adaptive sampler. The sampler calculates the RSS value on each frequency point, obtains an RSS profile $\vec{x}$ covering the bandwidth B, and periodically creates an RSS profile batch with all the RSS profiles in a period of T.

Although simple and straightforward, the basic sampling process has two issues. First, it cannot collect multiple samples of RSS profiles within a small range of locations while the vehicle is moving at different speeds, which is needed to cancel the white noise (*i.e.*, **Practical issue 1**). Second, the bandwidth of in-vehicle radio limits the number of radio stations covered in RSS profiles, which may affect the accuracy of the localization results (*i.e.*, **Practical issue 2**). To this end, RadioLoc introduces two novel mechanisms to address these issues, respectively.

Adaptive batching: The high mobility of vehicles is always a concern of localization and navigation systems. Fortunately, the impact of the Doppler shift is small enough to be neglected in our design. A straightforward calculation tells us that the Doppler shift is 20Hz for a $216km/h$ vehicle speed at the $100\ MHz$ FM frequency band.

We consider another issue brought by the high speed of vehicles, and propose a practical solution for it. Consider the batching technique described in Section III, which packages the RSS profiles as one batch every T seconds. Suppose there is a vehicle driving with the speed of v m/s. In this case, each batch of RSS profiles is recorded during a journey of vT meters. Depending on the variable v, the RSS profiles may correspond to very different physical distances, even if they were recorded from the same starting position. The RadioLoc system could suffer from these variations in the distance resolution. For example, it may compare real-time batches with a 20m distance to fingerprint batches with a

2m distance, and thus yield inconsistent results. To avoid this issue, we propose to adaptively adjust the period of each profile batch according to the vehicle's speed. Suppose the required resolution of distance is d (Without any further explanation, d is set to 3 meters in the rest of this paper.). Then the batch period is online adjusted as $T = d/v$ seconds. For instance, when the speed is 10 m/s (*i.e.*, 36 km/h), each batch will contain RSS profiles recorded in 0.3 seconds. When the speed increases to 20 m/s (*i.e.*, 72 km/h), the batch period reduces to 0.15 seconds. Both batches still cover the same distance of 3 meters. As such, *Practical Issue 1* is addressed.

Frequency sweep: The number of peaks (*i.e.*, radio stations) captured in each RSS profile determines the bandwidth B of the received FM signals. For some low-end FM radios, the bandwidth B may be too small to cover an abundant number of radio stations. The localization accuracy could be unsatisfactory in this case. To overcome this issue, we propose to adopt frequency sweep to enlarge the bandwidth. Support the desired bandwidth is $B_d > B$, starting from the lowest frequency of f_C. Then the FM radio will switch its center frequency one by one to cover the following frequencies: $\{f_C, f_C + B, f_C + 2B, \ldots, f_C + \lceil B_d/B \rceil B\}$. Therefore, with a sweep of $\lceil B_d/B \rceil$ narrowband samples, we can construct a virtual wideband RSS profile by concatenating them on the frequency domain. Note that in this case, the batch period is still the same as T seconds, but the number of wideband RSS profiles in each batch reduces to $RT/\lceil B_d/B \rceil$. As such, we address *Practical Issue 2*.

B. Data Processing: The Denoiser

The data processing component of RadioLoc consists of two novel modules. We first give the details of the denoiser, which eliminates the white noises in the RSS profiles as well as the signal distortions introduced by multipath delay spread. In particular, the denoiser consists of a Mahalanobis distance based filter and an rPCA denoising module. With these two novel techniques, RadioLoc removes the distortions caused by delay spreads as well as other noises, and thus addresses **Challenge 1**.

1) Mahalanobis Distance Based Filter: As previously illustrated in Fig. 2, an interesting observation of multipath delay spreads is that these spreads lead to large RSS variances around the station frequencies. This motivates us to pinpoint the distortions caused by delay spreads via detecting the frequency locations of high RSS variances. Concretely, we consider these high-variance points as outliers, and filter them out by detecting RSS values that are far away from the average distribution. We employ the Mahalanobis distance, as it quantifies the distance between a point and a distribution. The working procedure of the corresponding Mahalanobis distance based filter is described as Algorithm 1. Here, ρ is the empirical percentage of outliers, and is selected as 5% in this paper.

2) rPCA Denoising Module: To further clean the RSS profiles $\vec{Y}_M$, we develop a reconstructive PCA denoising technique. The corresponding rPCA denoising module analyzes the Principle Components (PCs) of the batch $\vec{Y}_M$, removes the most noisy one among these PCs, and reconstructs the profiles with the remaining ones as $\vec{Y}$. In this way, random noises and residual distortions are reduced. This procedure is described as Algorithm 2.

Algorithm 1 Mahalanobis Distance Based Filtering

Input: A batch of RSS profiles $\vec{X}$ consisting of N samples, and the empirical percentage ρ of outliers.
Output: A batch of filtered profiles $\vec{Y}_M$.
Step 1: Calculate the distribution of variances in RSS values on each frequency point as follows.
for $l = 1$ to L **do**
  $\overline{x}_{f_l} = \sum_{i=1}^{N} x_{f_l}^{(i)}/N$.
  $v_l = \sum_{i=1}^{N} (x_{f_l}^{(i)} - \overline{x}_{f_l})^2/N$.
end for
Step 2: Calculate the Mahalanobis distances of all $\{v_l, l = 1, \ldots, L\}$ as follows.
  $\mu = \sum_{l=1}^{L} v_l/L$.
  $\delta = \left(\sum_{l=1}^{L}(v_l - \mu)^2/L\right)^{1/2}$.
for $l = 1$ to L **do**
  Calculate the Mahalanobis distance as
  $\gamma_l = \left((v_l - \mu)(\delta^2)^{-1}(v_l - \mu)\right)^{1/2}$.
end for
Step 3: Remove outliers based on the Mahalanobis distances as follows.
Collect the largest $\lceil \rho L \rceil$ Mahalanobis distances, and put them into a set Γ.
$\gamma_{th} = \min\{\gamma_l | \gamma_l \in \Gamma\}$.
for $l = 1$ to L **do**
  if $\gamma_l >= \gamma_{th}$ **then** $y_{f_l}^{(i)} = 0,\ \forall i = 1, \ldots, N$.
  else $y_{f_l}^{(i)} = x_{f_l}^{(i)},\ \forall i = 1, \ldots, N$.
  end if
end for
Step 4: Output $\vec{Y}_M = \{\vec{y}^{(1)}, \ldots, \vec{y}^{(N)}\}$.

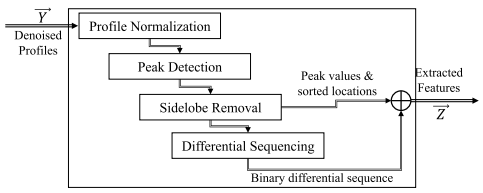

Fig. 5. Architecture of the feature extractor.

Note that this rPCA denoising technique is also able to remove the distortions brought by delay spread, since it can effectively eliminate high-variance elements from the profiles. However, it is hard to determine the PCs corresponding to the distortions in advance. Therefore, we develop the Mahalanobis distance based filter instead, and employ this rPCA denoising technique for other kinds of noises.

C. Data Processing: The Feature Extractor

After the noises in RSS profiles are eliminated, we next design a feature extractor to eliminate the FM signal inconsistency brought by the diversities of vehicles, radios, and weather conditions (*i.e.*, **Challenge 2** and **Challenge 3**). Fig. 5 presents the architecture of the feature extractor.

1) Profile Normalization: As investigated in Section II-B, the device diversity may introduce an unknown power offset to the FM signals, leading to inconsistent RSS profiles among different vehicles. In addition, drivers and passengers

Algorithm 2 rPCA Denoising

Input: A batch of RSS profiles $\vec{Y}_M$ consisting of N samples.
Output: A batch of denoised RSS profiles $\vec{Y}$.
Step 1: Conduct standard PCA on $\vec{Y}_M$, and achieve the PC coefficient matrix, $\vec{C}$, the PC score vector $vecS$, and the estimated means $\vec{M}$ as follows.

1: The PC coefficient matrix: $\vec{C} = \{\vec{c}_1, \ldots, \vec{c}_L\}$, where $\vec{c}_l$ is of length L and is the coefficient vector of the lth PC, and $\{\vec{c}_l\}$ are in descending order of component variance.
2: The PC score matrix: $\vec{S} = \{\vec{s}_1, \ldots, \vec{s}_L\}$, where $\vec{s}_l$ is of length N and is the score vector the lth PC.
3: The estimated means: $\vec{m} = \{m_1, \ldots, m_L\}^T$, where m_l is the estimated RSS mean at the lth frequency point.

Step 2: Extend the vector of the estimated means into a matrix as $\vec{M} = \underbrace{\{\vec{m}, \ldots, \vec{m}\}}_{N}$.
Step 3: Filter the PC with the largest variance as follows.

4: The filter coefficient matrix: $\hat{C} = \{\vec{0}, \ldots, \vec{c}_L\}$, where $\vec{0}$ is a zero vector of length L.
5: The PC score matrix: $\hat{S} = \{\vec{0}, \ldots, \vec{s}_L\}$, where $\vec{0}$ is a zero vector of length N.

Step 4: Reconstruct the RSS profiles as $\vec{Y} = \hat{C}\hat{S}^T + \vec{M}$, and output $\vec{Y}$.

Algorithm 3 Light-Weight Sidelobe Removal

Input: A vector of detected peaks $\vec{P}$, their corresponding frequencies $\vec{F}$, a length of frequency window B_W, and a threshold ratio β.
Output: Sidelobe removal results $\hat{P}$ and $\hat{F}$.
Step 1: Take the first element in $\vec{P}$ as the current element, denoted with subscript c.
Step 2: Collect all the peaks whose frequencies are inside the range of $[f_c^p - B_W, f_c^p + B_W]$, and put them into set W.
Step 3: Check sidelobes in W.

1: **for** $\forall \tilde{z}_l \in W$ **do**
2: **if** $\tilde{z}_l / \tilde{z}_c \leq \beta$ **then** Remove $\tilde{z}_l$ from $\vec{P}$, and remove f_1^p from $\vec{F}$
3: **end if**
4: **end for**

Step 4: Repeat step 2 and step 3 for the next element in $\vec{P}$. Upon reaching the end of $\vec{P}$, collect the remaining elements in $\vec{P}$ and $\vec{F}$, conduct zero-padding at the ends of them to make sure their lengths equal K, and output the padding results as $\hat{P}$ and $\hat{F}$, respectively.

may also adjust the power gains of in-vehicle radios, which also contributes to this unknown power offset. Such offsets are frequency non-selective. Therefore, the feature extractor minimizes the impact of these offsets by normalizing each RSS profile in $\vec{Y}$, and achieves the normalized profiles as $\overline{Z} = \{\overline{z}^{(1)}, \ldots, \overline{z}^{(N)}\}$, where $\overline{z}^{(i)}$ is the normalized version of $\vec{y}^{(i)}$ with a range of $[0, 1]$. This normalization is able to address Challenge 2 and Challenge 3 partially.

2) Peak Detection and Sidelobe Removal: To fully address these two challenges, we need to extract FM features that are irrelevant to the diversities of vehicles, radios, and weather conditions. To this end, we resolve to the appearances of different radio stations, as well as their relative order in RSS. The reasons are as follows. At a certain location, the number of radio stations and their frequencies inside a fixed bandwidth should be the same, regardless of the reception hardware and weather conditions. In case low-end radios lose a few stations to the noise, we further extract the relative order of these stations with respect to RSS values. In this way, high-end and low-end radios will always share most part in their orders of station RSS values.

To extract these features, the extractor first calculates the mean RSS value at each frequency point for all profiles in $\overline{Z}$:

$$\tilde{z}_{f_l} = \frac{1}{N} \sum_{i=1}^{N} y_{f_l}^{(i)}, \quad l = 1, \ldots, L, \tag{2}$$

and denote $\tilde{Z} = \{\tilde{z}_{f_1}, \ldots, \tilde{z}_{f_1}, \ldots, \tilde{z}_{f_L}\}^T$. The extractor then finds the largest K peaks in $\tilde{Z}$ and their corresponding locations, by applying the peak detection algorithm proposed by Du *et al.* in [18]. The RSS values of the peaks are recorded in a descending order as $\vec{P} = \{\tilde{z}_1, \ldots, \tilde{z}_K\}^T$. The frequencies corresponding to these peaks are also recorded as $\vec{F} = \{f_1^p, \ldots, f_K^p\}^T$. If the number of detected peaks is less than K, the extractor performs zero-padding at the ends of both $\vec{P}$ and $\vec{F}$.

However, the peaks recorded in $\vec{P}$ do not always correspond to the main lobes of radio stations. They may include sidelobes that are introduced by the finite FFT in digital signal processing. Detecting the sidelobes exactly is computationally complex. Therefore, we resolve to a light-weight algorithm to remove the sidelobes from $\vec{P}$ and $\vec{F}$, as described in Algorithm 3.

3) Binary Differential Sequencing: Besides the peaks, RadioLoc also leverages the shape of the profiles as another set of features. RadioLoc treats each profile as a series in the frequency domain, and extracts its evolving trend along with frequency. We utilize the differential sequence of each profile along frequency to capture how the RSS values evolve. The generation of this differential sequence is described as, for $l = 1, \ldots, L-1$,

$$\hat{d}_l = \begin{cases} 1, & \tilde{z}_{f_{l+1}} - \tilde{z}_{f_1} \geq 0, \\ 0, & \text{otherwise.} \end{cases} \tag{3}$$

We denote $\hat{D} = \{\hat{d}_1, \ldots, \hat{d}_{L-1}\}^T$. We adopt a binary differential sequence, because the magnitude information has already been captured in the peaks $\hat{P}$. Using a binary format allows us to minimize the data storage overhead without much degradation on the localization performance.

4) Weighting the Features: After feature extracting, we obtain two kinds of features, the peak-relating features $\hat{P}$ and $\hat{F}$, and the trend-relating features $\hat{D}$. The number of peak-relating features is much less than that of trend-relating features. However, peak-relating features may carry more important information about the RSS profiles. This information would be overwhelmed by trend-relating features in the learning process, if we directly merge all features into one set. Therefore, we adopt a weighting method to make sure that all kinds of features will be treated equivalently regardless of their numbers. The weight vector of

weights is described as

$$\hat{W} = \{w_1^P, \ldots, w_K^P, w_1^F, \ldots, w_K^F, w_1^D, \ldots, w_{L-1}^D\}^T, \quad (4)$$

where $\{w_i^P\}$ are the weights for $\hat{P}$, $\{w_i^F\}$ are the weights for $\hat{F}$, and $\{w_i^D\}$ are the weights for $\hat{D}$. An example implementation of these weights is

$$w_i^P = 1/K, i = 1, \quad \ldots, K, \quad (5)$$
$$w_i^F = 1/K, i = 1, \quad \ldots, K, \quad (6)$$
$$w_i^D = 1/(L-1), i = 1, \quad \ldots, l-1. \quad (7)$$

The final output of the whole feature extractor is

$$\vec{Z} = \{\hat{P}^T, \hat{F}^T, \hat{D}^T, \hat{W}^T\}^T. \quad (8)$$

D. Location Computation

After denoising the RSS profiles and extracting features that are uncorrelated to the diversities of vehicles, radios and weather conditions, the location computation component in RadioLoc takes in the extracted feature vector $\vec{Z}$, and outputs the 3D positions of vehicle (*i.e.*, longitude, latitude and altitude). To compute the accurate vehicle location swiftly, we resort to modern machine learning theories. In particular, we model the 3D localization of vehicle as a classification problem. This formulation is decoupled from the signal sampling and data processing components, hence allowing different machine learning algorithms to be plugged in.

To be concrete, in the location computation component, we first collect a set of RSS profiles and their corresponding ground truth 3D positions, use the denoiser and feature extractor to transform each RSS profile into a feature vector, and construct a training dataset $\mathbf{S}$ as the set of resulting (feature vector, 3D position) tuples. We leave the implementation details on how to collect the RSS profiles and the ground truth positions in Section V. We then use this training dataset to train a classifier $G(\vec{Z})$, which takes in the feature vector of an input RSS profile and outputs the corresponding 3D position.

Different learning algorithms can be deployed in RadioLoc due to its modular design. In our development, we implement several learning algorithms based on different machine learning theories (*e.g.*, random forest, SVM and AdaBoost) to compute the 3D positions of vehicles. We next present a random forest based 3D location learning algorithm as a proof of concept, and omit the details of other algorithms due to the space limit.

A random forest based 3D position identifier. Algorithm 4 gives the pseudo code of the random forested based 3D position identifier. Specifically, given a training dataset $\mathbf{S}$, the identifier first generates Θ smaller training datasets, each of which $\mathbf{S}_a$ is generated by randomly select samples from $\mathbf{S}$ with repetition (Line 10). For each dataset $\mathbf{S}_a$, the identifier trains a decision tree (Line 15-20). As a result, the random forest classifier G consists of a total of Θ decision trees (Line 11). When the identifier receives a new feature extractor $\vec{Z}$, G iterates through all its decision trees, gets all Θ 3D locations q_a computed by the trees, and returns the majority of $\{q_i\}$ as the final identification output (Line 1-5). In case of a draw, one of the majorities will be randomly selected as the output.

Algorithm 4 A Random Forest Based 3D Position Identifier

1: **procedure** POSITIONIDENTIFIER($\vec{Z}$)
2: **for** each decision tree t_a in G **do**
3: $q_a = t_a(\vec{Z})$
4: **end for**
5: Return the majority of $\{q_a\}_a$ as the final localization result
6: **end procedure**
7: **procedure** RANDOMFORESTCONSTRUCTION($\mathbf{S}$)
8: $G = \emptyset$
9: **for** $a = 1, \ldots, \Theta$ **do**
10: Random select samples from $\mathbf{S}$ with repetition to generate a new sample set $\mathbf{S}_a$
11: Add DECISIONTREELEARN($\mathbf{S}^a$) to G
12: **end for**
13: Return the forest G
14: **end procedure**
15: **procedure** DECISIONTREELEARN($\mathbf{S}$)
16: At each node:
17: Randomly select a small subset of features
18: Split on the best feature in the selected features
19: Return the learnt decision tree
20: **end procedure**

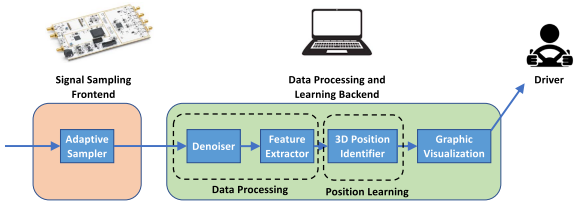

Fig. 6. The RadioLoc implementation.

V. IMPLEMENTATION AND DEPLOYMENT

In this section, we describe the implementation of a RadioLoc prototype, and the deployment settings of our field experiments using private vehicles.

A. RadioLoc Prototype Implementation

Figure 6 shows the RadioLoc prototype implementation. To avoid intrusive modifications to the test vehicles and obey local regulations on car tunings, the RadoLoc prototype is implemented on a USRP B210 software-defined radio board [19] and a commodity laptop. In particular, an adaptive sampler is implemented using GNURadio [20] on the USRP board as the signal sampling frontend to collect the raw RSS profiles of FM signals. These raw RSS profiles are then sent to the RadioLoc backend on the laptop, and processed through the denoiser and feature extractor before being sent to the 3D position identifier. The position identifier computes the vehicle's 3D location, and outputs the result to a graphic map interface. The whole data processing and learning backend is implemented in Python 3.7, with a total of ∼500 lines of code (LoC).

B. Test Deployment

We deploy our prototype of RadioLoc on three different vehicles to evaluate the impact of vehicle diversity. The first

(a) V1: Haval M2. (b) V2: Nissan Rogue. (c) V3: Volkswagen Bora.

Fig. 7. Vehicles employed in the experiments.

vehicle (denoted as V1) was a Great Wall Haval M2 SUV. The second vehicle (denoted as V2) is a Nissan Rogue SUV. The third vehicle (denoted as V3) is a Volkswagen Bora middle-size sedan. These three vehicles are owned and driven by three volunteering drivers, respectively.

Collection of FM Fingerprints Before being launched, RadioLoc needs to be trained with FM fingerprints of all positions of interest. Specifically, an FM fingerprint is the combination of its RSS profile and the corresponding ground truth 3D coordination. There are multiple approaches to collecting these FM fingerprints. We present two as examples in the following.

A first approach is to have location service providers drive their data collection vehicles (*e.g.*, Google street view vehicles) in different areas to collect the FM fingerprints. Specifically, these vehicles are equipped with an FM radio, a GPS device and a video camera. The GPS device collects rough coordination readings containing both horizontal and altitude errors, which are to be corrected with videos recorded by the camera. This can be done by setting up ground truth references in videos and interpolating the rest according to the vehicle speed. In this way, the ground truth coordinations are collected. The FM RSS profiles are then associated with these coordinations by aligning their synchronous time stamps, and the FM fingerprints are thus obtained.

Other than using vehicles designated for data collection, a second approach is to utilize crowdsourcing services. Drivers can collect and share their recorded FM fingerprints through mobile Apps such as Waze and Uber. Confidence levels can be applied to different users according to the resolution of their devices and the historical performance of their fingerprints. We note that the fingerprint collection process of RadioLoc does not affect the driving behavior of participating vehicles. The RSSI information is be automatically collected as the driver drives his vehicle. In contrast, earlier fingerprint-based FM-assisted localization methods require their system prototypes to stay at each collection point for at least 2 seconds to scan a large number of FM stations (*i.e.*, 32 [12], [21]). As a result, the fingerprints needed by these earlier methods cannot be collected via crowdsourcing services of vehicles.

In our experiments, we utilize the in-car Digital Video Recorders (DVRs) - the Jado D610s DVRs (Figure 8(a)), on the rear-view mirrors of both vehicles. The ground truth locations at each time slot are extracted from the recorded videos. These videos are synchronized to the portable FM radio, so that we can compare the results of RadioLoc with the ground truth. We also record GPS information with a GPS device - Garmin nuvi C265 (Figure 8(b)), which is also synchronized to the FM radio for comparison.

Scalability of RadioLoc. Theoretically, there are an infinite number of fingerprints in a global FM localization system. Putting them all together in one fingerprint library is non-scalable and infeasible. Instead, a distributed solution is described as follows. The urban areas are divided into hexagonal cells, each of which has its own identifier associated with a local library of FM fingerprints. Each vehicle determines

(a) Video recorder. (b) Garmin GPS.

Fig. 8. Additional devices used in the deployment to collect FM fingerprints.

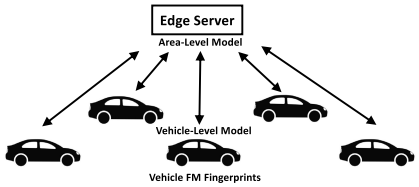

Fig. 9. The federated RadioLoc framework.

which cell it belongs to with the rough GPS readings, and adopts the FM fingerprints at that cell for localization. In case the vehicle is close to the edges of cells, it first determines the three closest cells, and prioritizes them according to the GPS distances from the vehicle to the centers of cells. The subsystem in each cell outputs an estimated position within its own fingerprint library, together with a confidence score (methods such as SVM and random forests all provide confidence scores). These confidence scores are then weighted by the priorities of the cells. The final position output is the one corresponding to the largest weighted confidence score. With this distributed solution, the proposed RadioLoc system can scale to a global level.

C. A Federated Framework of RadioLoc

Motivated by the recent progress in federated learning [22]–[24], we also extend the deployment RadioLoc with a federated framework (Figure 9). Compared with the earlier presented standalone mode, where vehicles collect FM fingerprints and send to a centralized server to train the localization model, federated RadioLoc allows vehicles to keep their FM fingerprints private to protect their sensitive information (*e.g.*, moving traces), while still provides the accurate, all-terrain localization service to vehicles.

In particular, given an area (*e.g.*, a street district), an edge server is deployed to store an area-level localization model. When a vehicle deployed RadioLoc drives into this area, it can retrieve the localization model from the edge server and use it for real-time localization.

The vehicle is also provided the option to participate in the federated training of the localization model in this area. If the vehicle chooses to participate, it first collects FM fingerprints as designed in Section V-B. It then uses the retrieved area-level localization model as the base, and uses its collected FM fingerprints to train its own vehicle-level localization model. Not only can this model be used by the vehicle itself for localization, it is also sent to the edge server. The latter then updates the area-level localization model by aggregating the received vehicle-level model. The specific model aggregation algorithm adopted by the edge server depends on which machine learning algorithm is used. For example, for SVM, the server can use the classic FedAvg algorithm [22] for model aggregation. For decision tree based algorithms (*e.g.*, Algorithm 4), we use the federated forest algorithm [23] to aggregate the decision trees built by different vehicles.

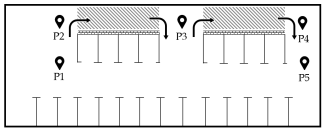

Fig. 10. Scenario 1: the floor plan of a parking building and the corresponding referencepoints.

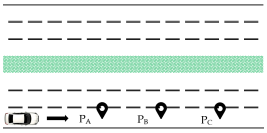

Fig. 11. Scenario 2: open street and the corresponding reference points.

VI. Experiment Methodology

In this section, we describe the experiment settings and the evaluation metrics.

A. Three Complementary Scenarios

The field experiments were conducted in three complementary real-life scenarios with different terrains.

Scenario 1 is a 3D scenarios used to evaluate the impact of diversities in vehicles and weather conditions. In order to achieve general conclusions, experiments in Scenario 1 may or may not have a clear view of sky, depending on the experiment positions. We choose a multi-level parking building to set up our experiments. This is because that, in the parking building, we can gather the ground truth data with 100% confidence. Moreover, we are able to repeat and reproduce the experiments exactly and safely without violating any traffic regulations.

The parking building has a total of four floors - three floors on the ground (denoted respectively as $1F$, $2F$ and $3F$) and one underground floor (denoted as $1B$). The height of each floor is 5 meters. On each floor, we select the same five horizontal positions ($P1$ to $P5$) as the reference points to gather FM data. We denote each reference point in Scenario 1 by its level and it horizontal position. For example, $P1$ on the second floor is denoted as $L2P1$. The horizontal floor plan of each floor is identical (except that $L3P2$ and $L3P4$ are both occupied by offices on the third floor), and is illustrated by Fig. 10. On each floor, $P2$ is at the entrance to the higher level, $P4$ is at the exit from the higher level, and $P3$ is between the entrance from the lower level and the exit to the lower level. $P2$, $P3$ and $P4$ are in a line, separated by 15 meters. $P1$ is 5 meters away from $P2$, and line $P1P2$ is perpendicular to line $P2P4$. The situation of $P5$ is similar to $P1$.

Scenarios 2 and 3 are used to evaluate the proposed system under dynamic environments. Scenario 2 concentrates on the impact of speed, and isolates other factors. Therefore, Scenario 1 is set up in an open and straight street with a clear view of sky. All field experiments in Scenario 2 are conducted at the same day. As illustrated by Fig. 11, we evaluate RadioLoc on a straight section of a 6-lane bi-directional street. There is no building (nor any sky-blocking object) within 100 meters of this section. In order to collect the ground truth for evaluation, we select three reference points (P_A, P_B, and P_C) locating on the midline of the rightmost lane. The distance between P_A and P_B, as well as that between P_B and P_C, is 5 meters. And the distance between P_A and P_C is 10 meters. During each run of experiments in Scenario 2, the same vehicle drives through this section with a constant speed, and passes the reference points in the order of P_A, P_B, and P_C.

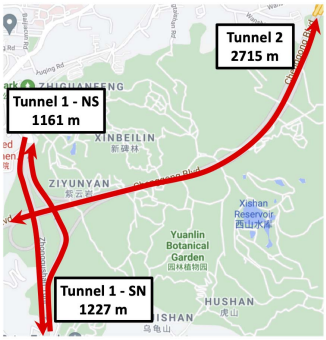

Fig. 12. The map of two tunnels, where the reference points are set every 5 meters.

Day	Scenario	Weather	Vehicle	Time
1	1	sunny	V1, V2	9:00
2	1	sunny	V1	12:30
3, 4	1	cloudy	V1	9:30, 22:00
5, 6	1	rainy	V1	16:30, 22:00
7	2	sunny	V2	23:00
8	3 (Tunnel 1)	cloudy	V3	14:00
8	3 (Tunnel 2)	cloudy	V3	17:00

Fig. 13. The summary of data collection.

In Scenario 3, we evaluate our proposed system under normal, *uncontrolled* driving behaviors in Xiamen, China, a tourist city with complex terrain environments. A driver drove through 2 mountain tunnels, denoted as Tunnel 1 and Tunnel 2, in both directions, in which no GPS signals can be received by the vehicle. The experiment in Tunnel 1 is performed at 2pm on a weekend day, representing the scenario of *normal traffic*. The experiment in Tunnel 2 is performed at 5pm the same day, representing the scenario of *heavy traffic*. We further note that Tunnel 1 was under road construction on the day of experiment. As such, its south-north route and north-south routes are asymmetric. Therefore, we separate the experiment in Tunnel 1 into two: denoted as Tunnel 1-SN and Tunnel 1-NS. Tunnel 1-SN is of 1227 meters long. Tunnel 1-NS is of 1161 meters long. Tunnel 2 is of 2715 meters long each way.

Scenarios 1, 2 and 3 are complementary to each other with different focuses. Scenario 1 concentrates on the impact of environment diversities. The impact of speed is neutralized due to the nature that vehicles in a parking building are either static or driving slowly. Scenario 2 focuses on the impact of vehicle speed, and eliminates the diversities in vehicles and weather conditions by conducting experiments in the same day with the same vehicle. Scenario 3 focuses on the real driving environments, where GPS signals are mostly unavailable.

B. Data Collection

The ground truth, the FM signal measurement and the GPS information are collected in seven days with either one or both vehicles. The weather of each day is either sunny, rainy or cloudy. For each weather condition, we repeat the measurement twice in two different days. Moreover, data collections are conducted either in the morning, at noon, in the afternoon or at night. The weather conditions, the number of vehicles, the scenarios of data collection and the collection time are summarized in Fig. 13. The numerical order of days in Fig. 13 is different from their calendar order.

During all experiments, the FM signal measurement is collected by drivers driving their vehicles through the reference points specified in Section VI-A and Figures 10, 11 and 12, without the need of stopping at any reference point. Each dataset consists of less than 20 data points per second. This is because RadioLoc only requires collecting the FM signals of one FM broadcast stations, as specified in Section V-B. This is different from, and much simpler than previous FM-based localization methods [12], [21], which require the device to stay at each reference point over 2 seconds to scan and collect the FM signals of 32 FM broadcast stations.

Furthermore, the size of our raw FM data shows that to perform all-terrain localization, the amount of data needed for a specific area is very small (*e.g.*, less than 10 MB for Tunnel-2 which is over 2.7 km). As such, with emerging storage techniques (*e.g.*, NVMe), RadioLoc can store FM signal data in vehicles with a low storage overhead.

C. Metrics

In this paper, we analyze the performance of localization systems from two different aspects.

On one hand, we evaluate whether a vehicle is correctly identified to the closest reference point. For many vehicular applications, identifying a vehicle to a reference point is as critical as (or even more important than) retrieving the exact coordination. For example, the ETC service needs to know not only the coordinations of nearby vehicles but also whether the vehicles are at the ETC gates. Also, even if errors exist, the navigation can still perform properly when vehicles are accurately located to critical references such as intersections and forks of roads, and levels of overpasses. Accordingly, the following metrics are adopted.

The **precision** of position identification for reference point i is defined as:

$$precision_i = \frac{tp_i}{tp_i + fp_i}, \tag{9}$$

where tp_i and fp_i are the numbers of true positives and false positives of reference point i, respectively. The average precision over all cases are then defined as:

$$\overline{precision} = \frac{1}{N}\sum_{i=1}^{N} precision_i, \tag{10}$$

where N is the number of reference points.

The **recall** of position identification of reference point i is defined as:

$$recall_i = \frac{tp_i}{tp_i + fn_i}, \tag{11}$$

where fn_i is the number of false negatives of reference point i. The average recall is then defined as:

$$\overline{recall} = \frac{1}{N}\sum_{i=1}^{N} recall_i. \tag{12}$$

In this paper, we consider the recall to be equivalent to the localization **accuracy**.

On the other hand, we are also interested in errors in the geometric space. A geometric error is defined as the Euclidean distance between the estimated coordination to the ground truth coordination. The average geometric **localization error** is then defined as:

$$\bar{\epsilon} = \frac{1}{N}\sum_{i=1}^{N}\sum_{i=j}^{N} P_{i,j} d_{i,j}, \tag{13}$$

where $P_{i,j}$ denotes the probability that vehicles at point i are identified to reference point j, $\sum_j^N P_i j = 1$, and $d_{i,j}$ denotes the Euclidean distance between i and j.

In addition to the above metrics, one may wonder how fast can RadioLoc localize the vehicle. In all of our experiments, our prototype is able to compute the location of the vehicle in less than 100 milliseconds. This demonstrates that RadioLoc is able to provide real-time vehicle localization. We omit the detailed results on localization latency due to the space limit.

	L_{-1}	L_1	L_2	L_3	recall
L_{-1}	30.2%	69.7%	0.1%	0.0%	30.2%
L_1	35.1%	64.2%	0.7%	0.0%	64.2%
L_2	20.7%	0.5%	78.8%	0.0%	78.8%
L_3	0.0%	31.7%	21.5%	46.8%	46.8%
precision	35.1%	38.7%	77.9%	100.0%	

Fig. 14. Confusion matrix of floor identification of RadioLoc **without** profile normalization.

Recall \ Training / Testing	Sunny	Rainy	Cloudy
Sunny	99.5%	73.1%	88.5%
Rainy	74.1%	99.2%	84.6%
Cloudy	85.2%	77.8%	99.6%

Fig. 15. Average recall of RadioLoc **without** feature extraction.

VII. Experiment Results Under Static Environments

In this section, we present the experiment results in Scenario 1, which represents the low-speed, mostly static environments. The purpose is to clearly illustrate the impacts of different factors with relatively clean settings.

A. The Impact of Multipath Delay Spread

We first evaluate whether the proposed denoiser is able to address the severe multipath reflections. We use the test data collected in Scenario 1, and focus on the geometric localization accuracy. Fig. 16 compares GPS, RadioLoc with a standard denoising technique [25], and RadioLoc with the proposed denoiser in terms of geometric errors. It is shown that RadioLoc can indeed improve the 3D localization accuracy over the existing GPS system. Furthermore, the standard denoising technique suffers from the severe multipath delay spread, leading to a maximum error of 15 meters (*i.e.*, wrong by 3 floors). This demonstrates the efficacy of the proposed rPCA-based denoiser in efficiently filtering out the noises and only leaving the signals from the FM station As such, it can minimize the impact of delay spread, and significantly reduces both the mean and maximum errors (*i.e.*, wrong by at most 1 floor). Therefore, RadioLoc is able to address **Challenge 1**.

B. The Impact of Diversity in Vehicle Models

In this section, we analyze the impact of vehicle diversity, and evaluate whether RadioLoc can work consistently across

Method \ Altitude error	mean	max
GPS	9.5 m	15.0 m
RadioLoc with a standard denoiser	2.9 m	15.0 m
RadioLoc with the proposed denoiser	0.3 m	5.0 m

Fig. 16. Geometric errors in Scenario 1.

	L_{-1}	L_1	L_2	L_3	recall
L_{-1}	99.5%	0.5%	0.0%	0.0%	99.5%
L_1	0.7%	99.3%	0.0%	0.0%	99.3%
L_2	0.0%	0.5%	99.5%	0.0%	99.5%
L_3	0.0%	0.0%	0.7%	99.3%	99.3%
precision	99.3%	99.0%	99.3%	100.0%	

Fig. 17. Confusion matrix of floor identification of RadioLoc **with** profile normalization.

TABLE II
CROSS VALIDATION OF IDENTIFICATION W/O PROFILE NORMALIZATION

Data being used	V1 only	V2 only	V1 and V2
Worst-case precision	99.8%	99.9%	35.1%
Worst-case recall	99.7%	100.0%	30.2%

different vehicle models. We evaluate the performance of altitude localization, and check whether the vehicles can be accurately located at the floor level. To this end, we use two datasets collected using V1 and V2, respectively, in Scenario 1 during Day 1. We then mix these data together. Recall that the feature extractor is proposed to address the vehicle diversity. Therefore, we compare RadioLoc systems with and without the profile normalization module. The confusion matricides are presented in Fig. 14 and Fig. 17, respectively.

As shown in Fig.14, without RSS profile normalization, there is a high chance that vehicles are located to a wrong floor. The worst-case precision and recall are 35.1% and 30.2%, respectively. Considering that there are a total of four floors, these results are only slightly better than random guesses.

To investigate the cause of this, we further evaluate the worst-case precision and recall using the data from only one vehicle in Table II. We can see that the cross validation results are nearly perfect when the data of only one vehicle is adopted. However, the performance of floor identification degrades significantly when it is applied to the mixed data from both vehicles. This again confirms the existence of Challenge 2. The diversity of vehicles may bring variations to path losses and receiver gains, making the raw FM RSS inconsistent.

On the other hand, when the normalization module is applied, the diversity of vehicles can be appropriately addressed. As shown in Fig. 17, the performance of floor identification improves largely even with a mix data from both vehicles. The worst-case precision and recall are raised to 99.0% and 99.3%, respectively. Moreover, it is shown that the error in floor identification is at most one floor. Hence, we conclude that the profile normalization addresses the power offsets brought by different vehicle models, and thus solves **Challenge 2**.

C. Impact of Weather Conditions

In this part, we evaluate RadioLoc under different weather conditions in Scenario 1. The experiments are conducted on six different days with three different weather conditions, *i.e.*, sunny, rainy and cloudy. For each weather condition,

Recall \ Training / Testing	Sunny	Rainy	Cloudy
Sunny	100%	99.6%	99.7%
Rainy	99.7%	100%	99.6%
Cloudy	99.7%	99.7%	100%

Fig. 18. Average recall of RadioLoc **with** feature extraction.

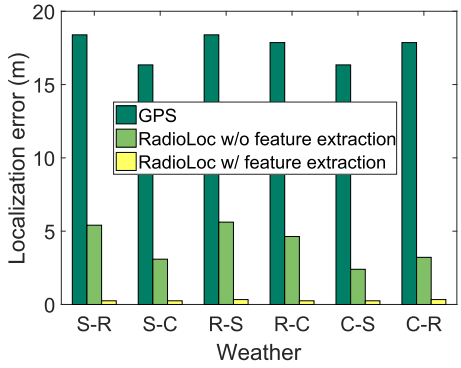

Fig. 19. Average 3D localization errors under different weather conditions in Scenario 1.

experiments are repeated twice on two different days. For Day 1, datasets from both vehicles are employed.

We first try to identify the positions of vehicles at the 18 reference points on four floors. Again, a weighted random forest is adopted as an example identifier. The evaluation is conducted as follows. 1) We first conduct the training with the data of a weather condition that is different from those of testing data. Each run of the evaluation mixed all data of one weather condition as the training data set, and considers the rest as testing data sets. The classifier is trained with the training data set, and is then tested separately on testing data sets. We denote the case of training on the sunny data set and testing on the rainy data set as the Sunny-Rainy pair (S-R for short). Similarly, the rest pairs are S-C, R-S, R-C, C-S, and C-R, respectively. 2) For pairs where the weather conditions are the same (*i.e.*, S-S, R-R, and C-C), we will take the data from one day as the training data, and consider the data from the other day with the same weather as the testing data.

After iterating through all training-testing pairs, we summarize the average recalls over all 18 reference points in Fig. 15. Note that the results in Fig. 15 are achieved using RSS profiles $\vec{Y}$ directly (*i.e.*, RadioLoc w/o feature extraction). In this case, when training and testing with the data from the same weather condition, the FM position identification can still perform quite well, even when the data are collected from two different days. However, when training on one weather condition and testing on others, the performance of position identification is not satisfactory. In the worst case, the vehicles have been located to wrong reference positions in 26.9% of the time. This suggests that the weather condition indeed brings variations to the FM fingerprints. Considering the fact that the profile normalization has been already applied, we can conclude that the fingerprint distortions happen not only in the scale but also in the shape of the signals.

To address this issue, we adopt the extracted features $\vec{Z}$ instead of the RSS profiles $\vec{Y}$. Field test results confirm that the extracted features are able to improve the accuracy of position identification. As illustrated in Fig. 18, the worst-case recall increases to 99.6% for training and testing under different weather conditions, and reaches 100.0% for training and testing on the same weather.

Method \ Altitude error	mean	max
GPS	9.5 m	15.0 m
RadioLoc-SVM with a standard denoiser	3.0 m	15.0 m
RadioLoc-SVM with the proposed denoiser	0.3 m	5.1 m

Fig. 20. RadioLoc-SVM: Geometric errors in Scenario 1.

	L_{-1}	L_1	L_2	L_3	recall
L_{-1}	99.0%	1.0%	0.0%	0.0%	99.0%
L_1	0.7%	99.2%	0.1%	0.0%	99.2%
L_2	0.0%	0.7%	99.3%	0.0%	99.3%
L_3	0.0%	0.0%	1.2%	98.8%	98.8%
precision	99.3%	98.3%	98.7%	100.0%	

Fig. 21. RadioLoc-SVM: Confusion matrix of floor identification with profile normalization.

Recall \ Training / Testing	Sunny	Rainy	Cloudy
Sunny	100%	99.1%	99.3%
Rainy	99.0%	100%	99.2%
Cloudy	98.9%	99.2%	100%

Fig. 22. RadioLoc-SVM: Average recall with feature extraction.

We further visualize the improvements brought by the feature extractor in Fig. 19. It is shown that the average geometric localization errors of GPS are always greater than 15 meters. These errors are reduced to less than 5 meters by RadioLoc without feature extraction. Moreover, using the extracted features helps RadioLoc lower the average errors to less than half a meter. Therefore, we conclude that the RadioLoc addresses **Challenge 3**.

D. Impact of Different Learning Methods

The results in earlier subsections focus on the RadioLoc prototype that uses the random forest based positioning algorithm presented in Section IV-D. To verify the modularity of RadioLoc, we also repeat all the earlier experiments on RadioLoc prototypes that use a linear kernel SVM positioning algorithm, and an AdaBoost based positioning algorithm. We find that these prototypes provide similar performances on all four major metrics (*i.e.*, about 1-5% performance fluctuation on precision, recall, accuracy and localization error). As an example, Fig. 20, Fig. 21 and Fig. 22 show the geometric errors, the confusion matrix of floor identification and the average recall of RadioLoc-SVM, a prototype using a linear kernel SVM positioning algorithm. Comparing them with the corresponding results of the prototype using the random forest based positioning algorithm (*i.e.*, Fig. 16, Fig. 17 and Fig. 18), we observe that the performance of RadioLoc-SVM is very similar, with a slight degradation. This finding demonstrates the efficiency and efficacy of the novel sampling and data processing mechanisms developed in RadioLoc. It also shows that the modularity of RadioLoc allows the plugin of different learning-based localization algorithms. As such, it paves the way for the wide deployment and adoption of RadioLoc. We omit the remaining figures due to the space limit.

VIII. Experiment Results Under Dynamic Environments

In this section, we push the system towards more realistic environment of our daily driving.

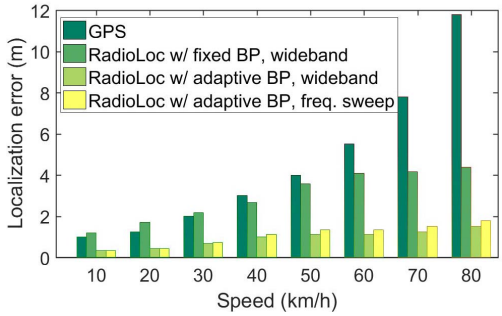

Fig. 23. Average horizontal localization errors under different velocities in Scenario 2.

A. Impact of Vehicle Speed

As discussed in Section II, the collected batches of FM profiles at the same reference point could be inconsistent under different speeds, undermining the performance of RadioLoc. To evaluate the impact of vehicle speed and the adaptive batching technique we proposed in Section IV-D to address this issue, we conduct multiple runs of tests in Scenario 2 with vehicle V2. At each run, V2 drives through three reference points, *i.e.*, P_A, P_B and P_C, in a straight line with a constant speed. Different speeds are adopted in different runs, ranging from $10km/h$ to $80km/h$. We first take the measurement data of $10km/h$ as the training data of a weighted random forest, and use the rest data to test the trained random forest. We then repeat this procedure for other speeds, and obtain the horizontal localization errors as shown in Fig. 23.

From Fig. 23, we can see that for all methods the localization errors increase with speed. Compared to GPS, RadioLoc largely reduces the localization errors in the high speed domain. However, when the speed is less than $40km/h$, RadioLoc with fixed batching period (Fixed BP) results in larger errors than those of GPS. This is caused by the inconsistency in FM fingerprints at different speeds. This issue is addressed by the use of adaptive batching period (Adaptive BP). As demonstrated in Fig. 23, the use of adaptive batching period helps reduce the average localization errors by at least 57.7%. In the worst case, the average localization error is less than 2 meters. In the high speed scenario of 80 km/h, RadioLoc with adaptive batching period reduces the average error to 16.7% of the GPS error. Thus, we conclude that the proposed RadioLoc system addresses *Practical Issue 1*.

In addition, we further compare the use of wideband FM signals to the use of frequency sweep, so as to approach the limits of RadioLoc with low-end devices. The bandwidth of the wideband radio is 10 MHz, while the bandwidth of the narrowband radio is 500 KHz. It is illustrated in Fig. 23 that the performance degradation brought by frequency sweep is small. The worst-case average localization error is still less than 2 meters. Therefore, we conclude that the proposed RadioLoc system addresses *Practical Issue 2*, and can be safely applied to existing FM radios on vehicles.

B. Driving Through Tunnels

As described before, in Scenario 3, a volunteer driver drove through 3 different routes, i.e., Tunnel 1 1-SN, Tunnel 1-NS and Tunnel 2, multiple times. For Tunnel 1-SN and Tunnel 1-NS, the driver repeated each route 6 times. For Tunnel 2, the driver repeated this route 10 times (5 times per direction). We asked the driver to drive as normal as possible,

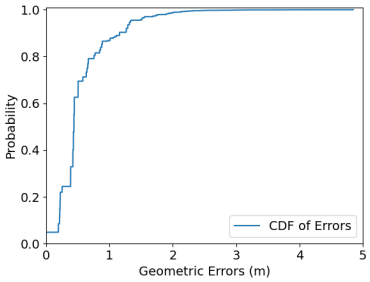

Fig. 24. RadioLoc errors in Tunnel 1-SN.

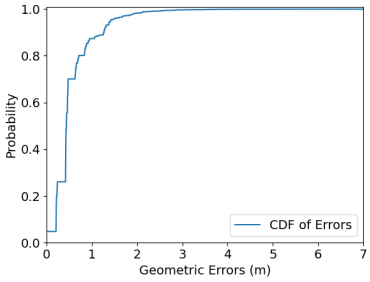

Fig. 25. RadioLoc errors in Tunnel 1-NS.

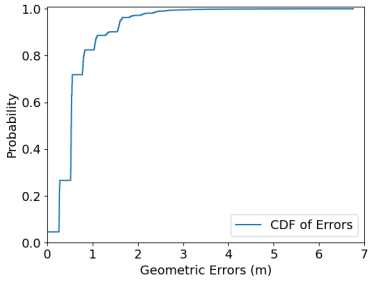

Fig. 26. RadioLoc errors in Tunnel 2.

and introduced no constraints on the driving behaviors (except obeying the speed limits and other traffic regulations). As a result, the speed of the vehicle changed dynamically during the experiments in an uncontrolled manner. The distribution of the speed during experiments in routes of Scenario 3 is illustrated by a Cumulative Probability Function (CDF) in Fig. 27.

For each route, we used 66.7% data as the training data, and tested on the rest 33.3% data. We repeated the model training and evaluation 5 times with 5 different random seeds. The geometric errors are reported in Table III. It is shown that RadioLoc is able to limit the mean geometric error to be smaller than 1 meter. Such an error performance is quite robust across different random seeds. In addition, RadioLoc constrains the worst-case errors to stay smaller than 10 meters most of the time. (Note that the GPS is unavailable when driving in tunnels, meaning that the GPS errors is infinite.)

We further illustrate the CDFs of the geometric errors at Tunnel 1-SN, Tunnel 1-NS and Tunnel 2 in Fig. 24, Fig. 25, and Fig. 26, respectively. From the above figures, we can see that 80% of the time, RadioLoc achieved an error that is smaller than 1 meter. And 95% of the time, RadioLoc obtained an error that is smaller than 2 meters. These results remain valid for all three routes. This again illustrates that RadioLoc is able to support vehicle localization and navigation at the areas, where GPS signals are not available.

We further recruit four more volunteer vehicles and let each driver drive through Tunnel 2 with normal behaviors 10 times.

TABLE III
GEOMETRIC ERRORS IN THE TUNNELS

Tunnels	Mean Error (m)	Max Error (m)
Tunnel 1-SN	0.58 ± 0.04	7.29 ± 3.00
Tunnel 1-NS	0.59 ± 0.05	5.92 ± 2.66
Tunnel 2	0.70 ± 0.05	8.32 ± 1.41
Tunnel 2 (federated RadioLoc)	0.75 ± 0.04	8.49 ± 1.63

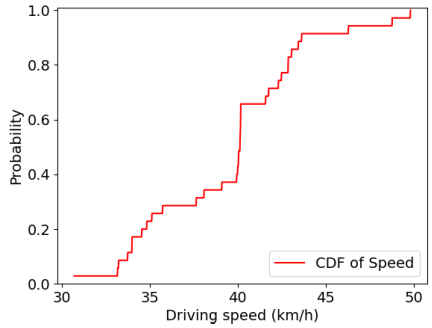

Fig. 27. CDF of speed during experiments in Scenario 3.

We use these four collected datasets and the earlier collected dataset of Tunnel 2 to construct a federation of five vehicles, and evaluate the performance of federated RadioLoc using the same methodology. The last line of Table III gives the average of geometric error of five vehicles. We see that the mean error is still within 0.75 meters. This demonstrates the feasibility of federated RadioLoc to achieve accurate localization without requiring the exposure of vehicles' FM fingerprints and moving traces.

IX. RELATED WORK

A. Global Positioning System

Equipped on over a billion smart phones and various devices such as digital cameras, sensors and etc., the global positioning system has become one of the most pervasive wireless technologies [26]. There has been a rich literature on how to improve the performance of GPS [2]–[4], [27]–[31], including quality, accuracy, delay and etc. To support the functionality of GPS under poor satellite signal conditions, most GPS receivers nowadays are embedded with other radios, such as WiFi, cellular and ZigBee. In this way, the content of the GPS signal can be downloaded from assisted GPS (A-GPS) servers instead of directly decoded from the satellite signals [2]–[4]. However, errors of A-GPS are significantly larger than those of standard GPS [4]. In addition, A-GPS requires GPS receivers to frequently re-synchronization with satellite signals, which is both time and energy consuming. Nee *et al.* propose the FFT-based GPS synchronization technique to reduce the complexity of this process from $O(n^2)$ to $O(n \lg(n))$ [27], where n is the number of samples per C/A code. Hassanieh *et al.* leverage this result and other advances in sparse FFT to further reduce the complexity to $O(n\sqrt{\lg(n)})$ [28].

B. LTE, WiFi and RFID Based Localization

Other than satellite, people also explore the potential and benefits of positioning with other wireless techniques [6], [7], [32]–[51]. Some representative ones are LTE, WiFi and radio

TABLE IV
COMPARISON BETWEEN RADIOLOC AND OTHER FM-ASSISTED LOCALIZATION METHODS

Method	Targeted Scenarios	Characteristics Used to Construct Signal Database	Collection Method	Accuracy
Chen *et al.* [12]	Indoor	FM RSSI, SNR, Multipath, and Frequency Offset	Stay 2 seconds at each reference point to scan 32 FM broadcast stations.	93% room-level accuracy (*i.e.*, 3-by-3 m^2), can be improved by using more, finer-grained reference points
Chen *et al.* [21]	Indoor	FM/WiFi RSSI, SNR, Multipath, and Frequency Offset	Stay 2 seconds at each reference point to scan 32 FM broadcast stations.	93% room-level accuracy (*i.e.*, 3-by-3 m^2), can be improved by using more, finer-grained reference points
Yoon *et al.* [14]	Indoor	FM RSSI	Synthesis by propagation model, using FM station information and building map.	89% room-level accuracy, an average error of 6 m error.
Youssef *et al.* [15]	Open road outdoor	FM RSSI	Drive through reference points to collect RSSI of 1 FM broadcast station.	An average of 8 km.
RadioLoc	All-terrain (*e.g.*, parking building, open road and tunnel)	FM RSSI	Drive through reference points to collect RSSI of 1 FM broadcast station.	An average error of $0.3m$ in parking building, $< 0.2m$ in open road, and $< 0.7m$ in tunnel.

frequency identification (RFID). The most popular approaches analyze the Angle of Arrival (AoA) or Time of Arrival (ToA) to determine the relative position of the receivers to the transmitters. For example, Kumar *et al.* propose the LTEye platform to monitor and analyze LTE radio performance at a fine granularity [32]. With the use of rotating antennas, LTEye is able to locate mobile users in an indoor environment. Xiong *et al.* propose ArrayTrack, a WiFi-based indoor localization system in which antenna arrays are installed at each access point to support the AoA based localization [6]. Kotaru *et al.* design SpotFi, a decimeter-level WiFi-based indoor localization system. One major advantage of SpotFi is that it does not require a large number of antennas to be installed on each access point, e.g., three antennas at each access point is sufficient to provide satisfying performance [34]. To avoid the cost and overhead of installing actual antenna arrays at access points [6], [32], [34], Kumar *et al.* propose Ubicarse, a system that constructs a virtual antenna array at a human-holding mobile device (e.g., a smart phone) by requiring the device owner to move the device in a circular fashion [7], and use the measurement from this virtual array to locate the device. Though Ubicarse does not require additional hardware modification, it relies on the existence of other in-device sensors such as accelerometers and gyroscopes to achieve accurate localization. Different from the above AoA localization scheme, Xiong *et al.* develop ToneTrack, a time-of-arrival based localization scheme [33]. Different from traditional ToA based solution, ToneTrack leverages the frequency agileness of WiFi to improve the bandwidth so that the localization accuracy can achieve sub-meter level. Subramanian *et al.* in [52] consider the problem from the other direction. They adopt directional antennas mounted on moving vehicles to collect WiFi AoA information for localization of roadside WiFi APs.

Some approaches also resolve to WiFi signal fingerprints such as RSS, and Channel State Information (CSI) for localization. Chintalapudi *et al.* in [53] adopts the RSS of WiFi as location fingerprints of devices, and develops an EZ Localization algorithm that captures the physical constraints of wireless propagation to setup fingerprints automatically. Wu *et al.* are able to utilize the fingerprints of WiFi CSI to enhance the accuracy indoor localization [5]. Yang *et al.* propose to model the FM signal distribution over the floors and use the collected fingerprint to perform indoor localization [13]. Yang *et al.* provide a comprehensive survey of WiFi fingerprint based indoor localization in [54].

Other than localization, WiFi fingerprints have also been applied to track 3D body movements through walls. WiVi [55] is such a system, which leverages MIMO communication and inverse synthetic aperture radar to identify simple gestures of people and their relative locations in a closed room. WiTrack is also designed to enable coarse-grained body part tracking without requiring user to carry any wireless devices [56]. Meanwhile, the Wisee system [57] analyzes the Doppler shifts in residential WiFi signals, and utilizes them to build WiFi fingerprints for gesture recognition in home environments. Recently, the Wikey system [58] is able to record fine-grained fingerprints of WiFi CSI-waveforms for keys on a keyboard, and recognizes keystrokes with these records.

Besides LTE and WiFi, fine-grained RFID localization methods are also explored. Tagoram uses COTS RFID tags and readers to track mobile RFID tags in real-time [38]. PinIt uses a moved antenna to measure the multipath pro- files of reference tags at known positions and locates the target RFID tag [39]. Though all these LTE, WiFi and RFID based systems enable accurate and low-cost localization of devices and users, they mostly target on an indoor scenario [59] and cannot support all-terrain 3D vehicle localization because (1) they usually require additional infrastructure and hardware modification and (2) they cannot cope with the highly dynamic vehicle environments.

C. FM-Assisted Localization

Recently, there has been a growing interest on FM-based localization methods [12]–[15]. Compared with the popular GPS or WiFi based approaches, FM radios consume less power and can cover a very large area. And existing methods also demonstrated that given a geographical area, the FM signal fingerprints are unique. Chen *et al.* demonstrate the feasibility of FM-RSS based localization. They show that the RSSI of FM radio signals can be used to achieve room-level indoor localization with similar or better accuracy to the one achieved by WiFi signals [12]. It is further revealed that when FM and WiFi signals are combined to generate wireless fingerprints, the localization accuracy can be significantly increased [21]. Matic *et al.* propose the spontaneous recalibration technique to reduce the delay caused by frequent calibration in FM-based

indoor localization systems [60]. Yoon *et al.* design ACMI, an FM-based indoor localization system requiring no proactive site profiling [14].

Though these systems demonstrate the benefits of FM-based localization. They are designed for indoor localization. FM-based all-terrain localization poses a series of unique challenges, such as the severe signal distortion caused by the rich multipaths in FM signal propagation, inconsistency of FM signals due to the diversities of vehicle models, radios, and weather conditions, the high mobility of vehicles, and the limited bandwidth of in-vehicle radios. And these challenges are not addressed in existing studies. For example, Youssef *et al.* explore the feasibility of the FM-modeling based technique in an outdoor setup [15] with a resolution of several kilometers. To the best of our knowledge, RadioLoc is the first working system that systematically addresses these issues to achieve efficient, accurate, all-terrain vehicle localization. In the end, we compare key aspects of RadioLoc and these related FM-assisted localization methods, in terms of their design decisions, applicability, and performance in Table IV.

X. Conclusion

We design RadioLoc, a novel system that uses the highly-available FM signal as the signal source and integrates modern machine learning techniques into the processing of FM signals to efficiently learn the accurate vehicle localization under all-terrain environments. A series of novel techniques are developed in RadioLoc to address the design challenges and practical issues in all-terrain vehicle localization. Field tests in real-life scenarios demonstrate that RadioLoc achieves a real-time localization latency with a worst-case accuracy of 99.6%.

References

[1] E.-R. Ahmed, *Introduction to GPS: The Global Positioning System* (Artech House Communication), vol. 6. New York, NY, USA: Library of Congress, 2002.

[2] J. LaMance, J. DeSalas, and J. Jarvinen, "Assisted GPS: A low-infrastructure approach," *GPS World*, vol. 13, no. 3, pp. 46–51, 2002.

[3] H. S. Ramos, T. Zhang, J. Liu, N. B. Priyantha, and A. Kansal, "LEAP: A low energy assisted GPS for trajectory-based services," in *Proc. 13th Int. Conf. Ubiquitous Comput.*, 2011, pp. 335–344.

[4] P. A. Zandbergen and S. J. Barbeau, "Positional accuracy of assisted GPS data from high-sensitivity GPS-enabled mobile phones," *J. Navigat.*, vol. 64, no. 3, pp. 381–399, 2011.

[5] K. Wu, J. Xiao, Y. Yi, D. Chen, X. Luo, and L. M. Ni, "CSI-based indoor localization," *IEEE Trans. Parallel Distrib. Syst.*, vol. 24, no. 7, pp. 1300–1309, Jul. 2013.

[6] J. Xiong and K. Jamieson, "ArrayTrack: A fine-grained indoor location system," in *Proc. NSDI*, 2013, pp. 71–84.

[7] S. Kumar, S. Gil, D. Katabi, and D. Rus, "Accurate indoor localization with zero start-up cost," in *Proc. 20th Annu. Int. Conf. Mobile Comput. Netw.*, Sep. 2014, pp. 483–494.

[8] Y. Xie, Z. Li, and M. Li, "Precise power delay profiling with commodity Wi-Fi," *IEEE Trans. Mobile Comput.*, vol. 18, no. 6, pp. 1342–1355, Jun. 2019.

[9] C. Zhang and X. Zhang, "Pulsar: Towards ubiquitous visible light localization," in *Proc. 23rd Annu. Int. Conf. Mobile Comput. Netw.*, Oct. 2017, pp. 208–221.

[10] T. Wei and X. Zhang, "Gyro in the air: Tracking 3D orientation of batteryless Internet-of-Things," in *Proc. 22nd Annu. Int. Conf. Mobile Comput. Netw.*, Oct. 2016, pp. 55–68.

[11] L. Li, P. Xie, and J. Wang, "RainbowLight: Towards low cost ambient light positioning with mobile phones," in *Proc. 24th Annu. Int. Conf. Mobile Comput. Netw.*, Oct. 2018, pp. 445–457.

[12] Y. Chen, D. Lymberopoulos, J. Liu, and B. Priyantha, "FM-based indoor localization," in *Proc. 10th Int. Conf. Mobile Syst., Appl., Services (MobiSys)*, 2012, pp. 169–182.

[13] Z. Yang, C. Wu, and Y. Liu, "Locating in fingerprint space: Wireless indoor localization with little human intervention," in *Proc. 18th Annu. Int. Conf. Mobile Comput. Netw. (Mobicom)*, 2012, pp. 269–280.

[14] S. Yoon, K. Lee, and I. Rhee, "FM-based indoor localization via automatic fingerprint DB construction and matching," in *Proc. 11th Annu. Int. Conf. Mobile Syst., Appl., Services (MobiSys)*, 2013, pp. 207–220.

[15] A. Youssef, J. Krumm, E. Miller, G. Cermak, and E. Horvitz, "Computing location from ambient FM radio signals [commercial radio station signals]," in *Proc. WCNC*, 2005, pp. 824–829.

[16] D. Kobak *et al.*, "Demixed principal component analysis of neural population data," in *Proc. NIPS*, 2016, p. e10989.

[17] F. Nan, J. Wang, and V. Saligrama, "Pruning random forests for prediction on a budget," in *Proc. NIPS*, 2016, pp. 2334–2342.

[18] P. Du, W. A. Kibbe, and S. M. Lin, "Improved peak detection in mass spectrum by incorporating continuous wavelet transform-based pattern matching," *Bioinformatics*, vol. 22, no. 17, pp. 2059–2065, 2006.

[19] *USRP b210 Radio Board*. Accessed: Sep. 1, 2020. [Online]. Available: https://www.ettus.com/all-products/ub210-kit/

[20] *GNU Radio*. Accessed: Oct. 1, 2020. [Online]. Available: https://www.gnuradio.org/

[21] Y. Chen, D. Lymberopoulos, J. Liu, and B. Priyantha, "Indoor localization using FM signals," *IEEE Trans. Mobile Comput.*, vol. 12, no. 8, pp. 1502–1517, Aug. 2013.

[22] K. Bonawitz *et al.*, "Towards federated learning at scale: System design," in *Proc. Mach. Learn. Syst.*, vol. 1, 2019, pp. 374–388.

[23] Y. Liu *et al.*, "Federated forest," *IEEE Trans. Big Data*, vol. 8, no. 3, pp. 843–854, Jun. 2022.

[24] L. A. C. de Souza, G. Antonio F. Rebello, G. F. Camilo, L. C. B. Guimaraes, and O. C. M. B. Duarte, "DFedForest: Decentralized federated forest," in *Proc. IEEE Int. Conf. Blockchain (Blockchain)*, Nov. 2020, pp. 90–97.

[25] S. V. Vaseghi, *Advanced Digital Signal Processing and Noise Reduction*. Hoboken, NJ, USA: Wiley, 2006.

[26] B. Hofmann-Wellenhof, H. Lichtenegger, and E. Wasle, *GNSS-Global Navigation Satellite Systems: GPS, GLONASS, Galileo, and More*. Cham, Switzerland: Springer, 2007.

[27] D. J. R. van Nee and A. J. R. M. Coenen, "New fast GPS code-acquisition technique using FFT," *Electron. Lett.*, vol. 27, no. 2, pp. 158–160, Jan. 1991.

[28] H. Hassanieh, F. Adib, D. Katabi, and P. Indyk, "Faster GPS via the sparse Fourier transform," in *Proc. 18th Annu. Int. Conf. Mobile Comput. Netw. (Mobicom)*, 2012, pp. 353–364.

[29] K. Zhang and P. Papadimitratos, "GNSS receiver tracking performance analysis under distance-decreasing attacks," in *Proc. ICL-GNSS*, 2015, pp. 1–6.

[30] M. Sahmoudi, M. G. Amin, and R. Landry, "Acquisition of weak GNSS signals using a new block averaging pre-processing," in *Proc. IEEE/ION Position, Location Navigat. Symp.*, 2008, pp. 1362–1372.

[31] J. B.-Y. Tsui, *Fundamentals of Global Positioning System Receivers*. Hoboken, NJ, USA: Wiley, 2000.

[32] S. Kumar, E. Hamed, D. Katabi, and L. E. Li, "LTE radio analytics made easy and accessible," in *Proc. ACM Conf. SIGCOMM*, Aug. 2014, pp. 211–222.

[33] J. Xiong, K. Sundaresan, and K. Jamieson, "ToneTrack: Leveraging frequency-agile radios for time-based indoor wireless localization," in *Proc. 21st Annu. Int. Conf. Mobile Comput. Netw.*, Sep. 2015, pp. 537–549.

[34] M. Kotaru, K. Joshi, D. Bharadia, and S. Katti, "SpotFi: Decimeter level localization using WiFi," in *Proc. ACM Conf. Special Interest Group Data Commun.*, Aug. 2015, pp. 269–282.

[35] N. O. Tippenhauer, K. B. Rasmussen, C. Pöpper, and S. Čapkun, "Attacks on public WLAN-based positioning," in *Proc. ACM/Usenix Int. Conf. Mobile Syst., Appl. Services (MobiSys)*, 2009, pp. 29–40.

[36] N. Banerjee, S. Agarwal, P. Bahl, R. Chandra, A. Wolman, and M. Corner, "Virtual compass: Relative positioning to sense mobile social interactions," in *Pervasive Computing*. Cham, Switzerland: Springer, 2010, pp. 1–21.

[37] H. Liu, J. Yang, S. Sidhom, Y. Wang, Y. Chen, and F. Ye, "Accurate WiFi based localization for smartphones using peer assistance," *IEEE Trans. Mobile Comput.*, vol. 13, no. 10, pp. 2199–2214, Oct. 2014.

[38] L. Yang, Y. Chen, X.-Y. Li, C. Xiao, M. Li, and Y. Liu, "Tagoram: Real-time tracking of mobile RFID tags to high precision using COTS devices," in *Proc. 20th Annu. Int. Conf. Mobile Comput. Netw.*, Sep. 2014, pp. 237–248.

[39] J. Wang and D. Katabi, "Dude, where's my card?: RFID positioning that works with multipath and non-line of sight," in *Proc. ACM SIGCOMM Conf. SIGCOMM*, Aug. 2013, pp. 51–62.
[40] D. Koutsonikolas, S. M. Das, and Y. C. Hu, "Path planning of mobile landmarks for localization in wireless sensor networks," *Comput. Commun.*, vol. 30, no. 3, pp. 2577–2592, 2007.
[41] T. Grosse-Puppendahl *et al.*, "Platypus: Indoor localization and identification through sensing of electric potential changes in human bodies," in *Proc. 14th Annu. Int. Conf. Mobile Syst., Appl., Services*, Jun. 2016, pp. 17–30.
[42] A. T. Mariakakis, S. Sen, J. Lee, and K.-H. Kim, "SAIL: Single access point-based indoor localization," in *Proc. 12th Annu. Int. Conf. Mobile Syst., Appl.*, Jun. 2014, pp. 315–328.
[43] C.-J. Huang, Y.-L. Wei, C. Fu, W.-H. Shen, H.-M. Tsai, and C.-J.-K. Lin, "LiBeamScanner: Accurate indoor positioning with sweeping light beam," in *Proc. 2nd Int. Workshop Visible Light Commun. Syst.*, Sep. 2015, pp. 33–38.
[44] Q. Xu, A. Gerber, Z. M. Mao, and J. Pang, "AccuLoc: Practical localization of performance measurements in 3G networks," in *Proc. 9th Int. Conf. Mobile Syst., Appl., Services (MobiSys)*, 2011, pp. 183–196.
[45] L. Li, G. Shen, C. Zhao, T. Moscibroda, J.-H. Lin, and F. Zhao, "Experiencing and handling the diversity in data density and environmental locality in an indoor positioning service," in *Proc. 20th Annu. Int. Conf. Mobile Comput. Netw.*, Sep. 2014, pp. 459–470.
[46] P. Hu, L. Li, C. Peng, G. Shen, and F. Zhao, "Pharos: Enable physical analytics through visible light based indoor localization," in *Proc. 12th ACM Workshop Hot Topics Netw.*, Nov. 2013, pp. 1–7.
[47] S. Rallapalli, L. Qiu, Y. Zhang, and Y.-C. Chen, "Exploiting temporal stability and low-rank structure for localization in mobile networks," in *Proc. 16th Annu. Int. Conf. Mobile Comput. Netw. (MobiCom)*, 2010, pp. 161–172.
[48] S. Sen, B. Radunovic, R. R. Choudhury, and T. Minka, "You are facing the Mona lisa: Spot localization using PHY layer information," in *Proc. 10th Int. Conf. Mobile Syst., Appl. (MobiSys)*, 2012, pp. 183–196, doi: 10.1145/2307636.2307654.
[49] D. Li, T. Bansal, Z. Lu, and P. Sinha, "MARVEL: Multiple antenna based relative vehicle localizer," in *Proc. 18th Annu. Int. Conf. Mobile Comput. Netw. (Mobicom)*, 2012, pp. 245–256.
[50] M. Li and Y. Liu, "Rendered path: Range-free localization in anisotropic sensor networks with holes," *IEEE/ACM Trans. Netw.*, vol. 18, no. 1, pp. 320–332, Feb. 2010.
[51] X. Shen, Y. Chen, J. Zhang, L. Wang, G. Dai, and T. He, "BarFi: Barometer-aided Wi-Fi floor localization using crowdsourcing," in *Proc. IEEE 12th Int. Conf. Mobile Ad Hoc Sensor Syst.*, Oct. 2015, pp. 416–424.
[52] A. P. Subramanian, P. Deshpande, J. Gao, and S. R. Das, "Drive-by localization of roadside wifi networks," in *Proc. 27th IEEE Int. Conf. Comput. Commun.*, 2008, pp. 718–725.
[53] K. Chintalapudi, A. Padmanabha Iyer, and V. N. Padmanabhan, "Indoor localization without the pain," in *Proc. 16th Annu. Int. Conf. Mobile Comput. Netw. (MobiCom)*, 2010, pp. 173–184.
[54] Z. Yang, Z. Zhou, and Y. Liu, "From RSSI to CSI: Indoor localization via channel response," *ACM Comput. Surveys*, vol. 46, no. 2, pp. 1–32, Nov. 2013.
[55] F. Adib and D. Katabi, "See through walls with WiFi!" in *Proc. ACM SIGCOMM Conf.*, Aug. 2013, pp. 75–86.
[56] F. Adib, Z. Kabelac, D. Katabi, and R. C. Miller, "3D tracking via body radio reflections," in *Proc. 11th USENIX Symp. Netw. Syst. Design Implement. (NSDI)*, 2014, pp. 317–329.
[57] Q. Pu, S. Gupta, S. Gollakota, and S. Patel, "Whole-home gesture recognition using wireless signals," in *Proc. 19th Annu. Int. Conf. Mobile Comput. Netw. (MobiCom)*, 2013, pp. 27–38.
[58] K. Ali, A. X. Liu, W. Wang, and M. Shahzad, "Keystroke recognition using WiFi signals," in *Proc. 21st Annu. Int. Conf. Mobile Comput. Netw.*, Sep. 2015, pp. 90–102.
[59] P. Bahl, "Indoor localization: Are we there yet?" *GetMobile, Mobile Comp. Commun.*, vol. 19, no. 1, pp. 25–28, 2015.
[60] A. Matic, A. Papliatseyeu, V. Osmani, and O. Mayora-Lbarra, "Tuning to your position: FM radio based indoor localization with spontaneous recalibration," in *Proc. IEEE Int. Conf. Pervas. Comput. Commun. (PerCom)*, Mar. 2010, pp. 153–161.

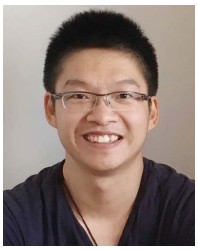

Xi Chen received the Ph.D. degree in computer science from McGill University, Canada, in 2017. He is a Senior Principal Scientist with Huawei Noah's Ark Laboratory, Montreal; and an Adjunct Professor with the School of Computer Science, McGill University. Before joining Huawei and McGill University, he was a Research Staff with Samsung and Nuance Communication Inc. His research interests include intelligent transportation systems, the Internet of Things, machine learning, and natural language processing.

Qiao Xiang (Member, IEEE) received the bachelor's degrees in information security and in economics from Nankai University in 2007 and the master's and Ph.D. degrees in computer science from Wayne State University in 2012 and 2014, respectively. From 2016 to 2016, he was a Post-Doctoral Fellow with the Department of Computer Science, Yale University. From 2014 to 2015, he was a Post-Doctoral Fellow with the School of Computer Science, McGill University. He was an Associate Research Scientist with the Department of Computer Science, Yale University. He is a Professor with Xiamen University. His research interests include software defined networking, resource discovery, and orchestration in collaborative data sciences; interdomain routing; and wireless cyber-physical systems.

Linghe Kong (Senior Member, IEEE) received the B.Eng. degree in automation from Xidian University in 2005, the master's degree in telecommunication from Telecom SudParis in 2007, and the Ph.D. degree in computer science from Shanghai Jiao Tong University in 2013. He is currently a Professor with the Department of Computer Science and Engineering, Shanghai Jiao Tong University. Before that, he was a Post-Doctoral Researcher with Columbia University, McGill University, and the Singapore University of Technology and Design. His research interests include wireless networks, big data, mobile computing, and the Internet of Things.

Huisan Xu received the bachelor's degree in computer science from Xiamen University, China, in 2022, where he is a graduate student with the Department of Computer Science. His research interests include networks verification, the Internet of Things, software-defined networking, and machine learning.

Xue Liu (Fellow, IEEE) received the Ph.D. degree (Hons.) in computer science from the University of Illinois at Urbana–Champaign, Champaign, IL, USA. He has also worked as the Samuel R. Thompson Chaired Associate Professor with the University of Nebraska–Lincoln and as a Visiting Faculty with HP Labs, Palo Alto, CA, USA. He is a William Dawson Scholar (Chair Professor) and a Full Professor with the School of Computer Science, McGill University, Montreal, Canada. His research interests include computer and communication networks, real-time and embedded systems, cyber-physical systems and the IoT, green computing, and smart energy technologies. He has published more than 200 research papers in major peer-reviewed international journals and conference proceedings in these areas and received several best paper awards. His research has been covered by various news media.